COMPARISON OF DIELECTRICS AND IODINE SOLUTION FOR MONOCRYSTALLINE AND MULTICRYSTALLINE SURFACE PASSIVATION

J. Brody[1], P. Geiger[2], G. Hahn[2], and A. Rohatgi[1]
1. Georgia Institute of Technology, Atlanta GA 30332-0250, USA
2. University of Konstanz, Department of Physics, Germany

ABSTRACT

The effective lifetimes of monocrystalline and multicrystalline wafers were measured under dielectric and iodine-solution surface passivation using inductively coupled photoconductance. While all 18 spots measured on monocrystalline materials had significantly higher (>10%) lifetimes under iodine passivation than dielectric passivation, this condition was satisfied by only 12 of 18 spots measured on cast multicrystalline wafers and just 6 of 18 spots measured on string ribbon. Possible reasons for this behavior are discussed in this paper. Moreover, the differences in surface passivation effectiveness have also been investigated with lifetime maps in order to overcome measurement problems related with the inhomogeneity of ribbon silicon.

1. INTRODUCTION

Material costs favor thinner devices that are more sensitive to surfaces; thus, the achievement of excellent surface passivation becomes increasingly important. Accordingly, there is a strong interest in the surface recombination velocity (S) conferred by various dielectric films on low-cost materials such as string ribbon silicon. A popular method for the determination of S involve the following steps: the effective lifetime (τ_{eff}) of a dielectric-passivated wafer is measured first. Next, the dielectric is removed, and the wafer is passivated in an iodine solution [1, 2] known to reduce surface recombination to very low levels on monocrystalline silicon. Neglecting recombination at the iodine-passivated surface, a subsequent lifetime measurement yields the bulk lifetime (τ_b). From these data, S under certain conditions (typically, $\tau_{eff} > 20\ \mu s$) can be determined by the equation

$$S = \frac{W}{2}\left(\frac{1}{\tau_{eff}} - \frac{1}{\tau_b}\right) = \frac{W}{2}\left(\frac{\tau_b - \tau_{eff}}{\tau_{eff}\,\tau_b}\right), \quad (1)$$

where W is the thickness of the wafer. For lower-lifetime wafers excited by slowly decaying illumination, the full steady-state solution to the continuity equation must be used [3].

For this method to work, the iodine solution must passivate the surface more effectively than the dielectric; in other words, the approximate measurement of τ_b (in the iodine solution) must be greater than τ_{eff} (with dielectric passivation) so that S > 0 will be calculated. However, previous work [4] has shown that four of eight sting ribbon wafers had better lifetimes when measured under dielectric passivation than iodine passivation. A possible explanation for this result is that the lifetimes were bulk-dominated under both dielectric and iodine passivation, rendering the measurements insensitive to S. If this is correct, then the apparent differences between iodine and dielectric passivation were due to measurement error.

2. EXPERIMENT

For a more comprehensive comparison of dielectric and iodine passivation on monocrystalline and multicrystalline materials, 35 wafers of various types and resistivities were coated according to one of several standard dielectric passivation schemes. A forming-gas anneal was performed on all wafers. Next, τ_{eff} was measured on one spot on each monocrystalline wafer and three spots on each multicrystalline wafer; photoconductance was determined by inductive coupling with a roughly 1-cm-diameter inductive coil. Finally, the dielectrics were removed, and the wafers were cleaned in standard chemical solutions, passivated in the iodine solution, and measured once again. To confirm the quality of the iodine solution used for all wafers, the lifetime of a high-resistivity float-zone wafer was measured during immersion in the solution, yielding 1.8 ms. This guarantees a maximum S of 8.5 cm/s at the iodine-passivated surface of this wafer.

Material quality in as-grown ribbon silicon usually varies quite strongly. Consequently, apart from inductively coupled measurements we were interested in measurements allowing a higher spatial resolution of lifetime distributions. The influence of different surface passivation schemes was therefore also investigated using the method of microwave-detected photoconductance decay (μ-PCD) with a spatial resolution of <1 mm.

3. RESULTS AND DISCUSSION

Table I indicates, for each material, the number of cases in which the lifetime measured during iodine passivation (τ_{iodine}) exceeded the lifetime measured on the same spot during dielectric passivation ($\tau_{dielectric}$). Using a suggested experimental uncertainty of 10% [5], $0.9\tau_{iodine} > 1.1\tau_{dielectric}$ must be satisfied to be confident that $\tau_{iodine} > \tau_{dielectric}$. While this condition is satisfied for all 18 monocrystalline wafers measured, it fails for one-third of the spots measured on the cast multicrystalline wafers and for two-thirds of the spots measured on the ribbon wafers. This suggests that equating τ_{iodine} with τ_b to calculate S must be used with caution for low-lifetime materials: in these, τ_{eff} for a dielectric could be dominated by τ_b instead of S, so that the method described above would fail and differences could be attributed to measurement errors.

This is especially true when as-grown ribbon samples are used, and τ_b is very low (≤3 µs). Furthermore, it has not yet been proven by using inductively coupled photoconductance that the iodine solution passivates these wafers more effectively than the dielectrics under investigation.

Although $\tau_{dielectric} \geq \tau_{iodine}$ was observed on four string ribbon wafers, the difference between the two lifetimes was always within measurement error in these cases. Thus, these data obtained from inductively coupled photoconductance do not suggest that dielectrics passivate more effectively than the well-known iodine solution.

Table I. Number of spots measured using inductively coupled photoconductance on each material satisfying the specified inequality. (Each cast and string ribbon wafer was measured on three spots, and the 5 web samples were measured under both oxide and oxide/nitride stack passivation.)

	$\tau_{iodine} > \tau_{dielectric}$	$0.9\tau_{iodine} > 1.1\tau_{dielectric}$
FZ	9 of 9	9 of 9
Cz	9 of 9	9 of 9
Cast	18 of 18	12 of 18
Ribbon	14 of 18	6 of 18
Web (oxide)	5 of 5	5 of 5
Web (stack)	3 of 5	3 of 5

In spite of our best efforts to measure the wafers at the same spots under dielectric and iodine passivation, the positioning may have varied slightly. Moreover, cast and especially ribbon silicon shows rather inhomogeneous material properties within small wafer areas. As a consequence, apart from further principal problems in measurement described in [7], integral lifetime measurements might partly incorporate bulk-dominated areas that would falsify the results of S determination. To address these concerns, area-integrated measurements were compared with lifetime maps as follows. Three 1.5 Ω-cm, p-type string ribbon silicon wafers were coated according to different passivation schemes: ~100 Å thermal oxide, ~850 Å PECVD silicon nitride deposited at 300°C, and a stack of nitride on top of oxide. The τ_{eff} of each wafer was measured in two ways: area-integrated measurements of four spots based on coupling with a roughly 1 cm-diameter inductive coil, and high-resolution lifetime mapping (< 1mm) performed with a microwave-detected PCD system under low-injection conditions using 1 sun bias light and a laser wavelength of 904 nm. Each mapping described in this paper is not a standard measurement but a reliable composition of various mappings performed with different time ranges in which the signal decay was evaluated [6, 7].
Next, the dielectrics were removed, and the wafers were cleaned and re-measured in an iodine solution. Area-integrated data are compared with average mapped values in Table II.

For typical as-grown lifetimes in the range of 1-10 µs, Table II suggests that oxide and the dielectric stack passivate string ribbon silicon as well as the iodine solution. In the case of silicon nitride, however, it can be seen that iodine tends to provide a better surface passivation than nitride. More detailed information can be

Table II. Mean τ_{eff} (µs) obtained by four area-integrated measurements (QSSPC, A) and lifetime map (µ-PCD, B).

	Dielectric (A)	**Iodine (A)**		**Dielectric (B)**	**Iodine (B)**
Nitride	1.4	1.8		1.8	2.1
Stack	3.0	2.6		3.0	2.9
Oxide	2.7	3.1		2.9	3.0

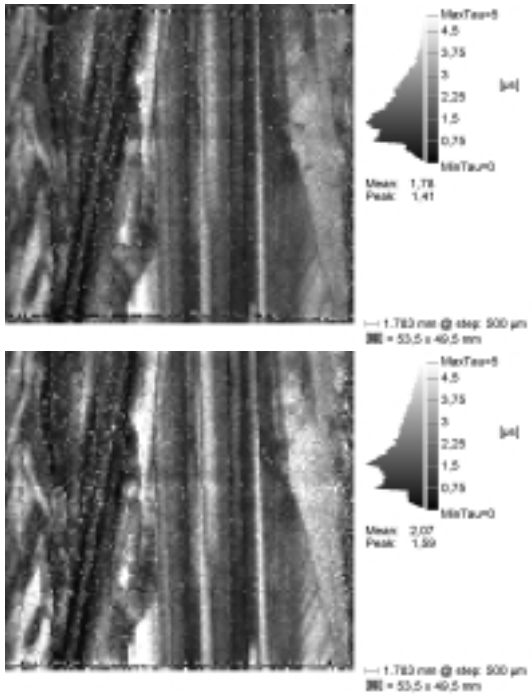

Fig. 1. µ-PCD lifetime maps obtained for a string ribbon wafer passivated by silicon nitride (upper map) and an iodine solution (lower map).

obtained by analyzing the corresponding lifetime maps given in Fig. 1. There it can be seen that differences between the two passivation methods are found especially in regions of higher lifetimes where bulk domination of τ_{eff} is less severe.

To get a more quantitative impression local mean values have been calculated for the nearly homogeneous wafer areas indicated in Fig. 2. In this way it is possible to compare the differences in effective lifetimes measured with both surface passivation techniques in regions with different bulk lifetime. As Table III shows, the differences get stronger the higher the measured effective lifetime values are. This is due to an increasing influence of surface recombination velocity on measured $\tau_{eff.}$ Consequently, it can be concluded from the µ-PCD data that the iodine solution passivates ribbon silicon more efficiently than silicon nitride. This makes it possible to determine local S values without the disturbing influence of the whole wafer's inhomogeneity.

The full solution to the steady-state continuity equation [3] is used to compute S for the nitride-coated ribbon surface in Table III; τ_b is taken to be τ_{iodine}. (Equation (1), an approximation valid only for low S, overestimates S in these cases. See [3] for details.) All four S values fall within 670-950cm/s. It thus appears that

the surface quality is much more uniform than τ_b, which ranges from 0.84-5.6 µs over the same four areas. While S on nitride-passivated monocrystalline materials can be as low as 4 cm/s [8], the values in Table III are less than or equal to the 950 cm/s reported for a ribbon sample in [9].

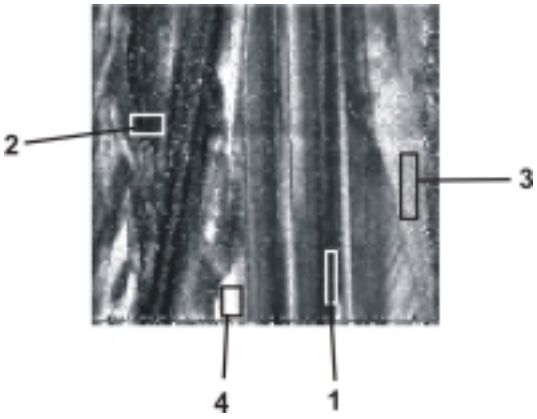

Fig. 2. Location of the four areas in which local lifetimes are computed and listed in Table III.

Table III. Local effective lifetimes computed for four small, nearly homogeneous areas of a string ribbon wafer. Low-lifetime areas appear dominated by bulk recombination regardless of surface passivation, while higher-lifetime areas show significantly different lifetimes under nitride and iodine passivation.

	$\tau_{nitride}$ (µs)	τ_{iodine} (µs)	$\tau_{nitride}/\tau_{iodine}$	S (cm/s)
Area 1	0.77	0.84	.92	950
Area 2	1.0	1.1	.91	850
Area 3	3.0	3.6	.84	670
Area 4	4.1	5.6	.72	850

4. CONCLUSIONS

While integral QSSPC measurements are well suited to determine S in monocrystalline Si wafers, they do not provide reliable results in the case of as-grown multicrystalline silicon ribbons because of varying material quality.

For the calculation of S it is necessary that the iodine solution provides a better surface passivation than the dielectrics. With the help of spatially resolved µ-PCD measurements it could be shown that an iodine solution provides better surface passivation than silicon nitride on as-grown ribbon silicon wafers, whereas no significant differences have been found in comparison to silicon oxide or nitride/oxide stacks in lifetime ranges of 1-10 µs.

The evaluation of S in the case of silicon nitride is possible when effective lifetimes are determined with a higher resolution by using µ-PCD measurements. Here effective lifetimes can be locally integrated in small areas of rather homogeneous quality and accurate results for S can be obtained.

REFERENCES

1. A.W. Stephens, M.A. Green, Solar Energy Materials & Solar Cells 45 (1997), pp. 255-265.
2. H. M'Saad, J. Michel, J. J. Lappe, L. C. Kimerling, J. Electronic Mat. 23 (1994), pp. 487-491.
3. J. Brody, A. Rohatgi, A. Ristow, Solar Energy Materials & Solar Cells **77** (2003), pp. 293-301.
4. J. Brody, A. Rohatgi, Proc. of the 29th IEEE PVSC, 2002, pp. 53-57.
5. M. Bail and R. Brendel, Proc. of the 16th EC PVSEC, 2000, pp. 98-101.
6. P. Geiger, G. Kragler, G. Hahn, P. Fath, E. Bucher, Proc. of the 29th IEEE PVSC, 2002, pp. 186-189.
7. P. Geiger, G. Kragler, G. Hahn, P. Fath, E. Bucher, Proc. of the 17th EC PVSEC, 2001, pp. 1754-1757.
8. T. Lauinger, J. Schmidt, A. G. Aberle, R. Hezel, Appl. Phys. Lett. **68** (1996), pp. 1232-4.
9. H. Morita, A. Sato, H. Washida, T. Kato, A. Oneo, Japanese J. of Appl. Phys. **21** (1982), pp. 47-51.